Light Intensity and Charge Holding Time Dependence of Pinned Photodiode Full Well Capacity

Ken Miyauchi[1, 2], Toshiyuki Isozaki[1], Rimon Ikeno[1] and Junichi Nakamura[1]

[1]Brillnics Japan Inc., Tokyo, Japan [2]Graduate School of Engineering, Tohoku University, Sendai, Japan

Contact: Ken Miyauchi: phone:+81-3-6404-8066, fax:+81-3-5767-5568,

email: miyauchi.ken@brillnics.com[1], miyauchi.ken.s1@dc.tohoku.ac.jp[2]

In this paper, light intensity and charge holding time dependence of pinned photodiode (PPD) full well capacity (FWC) are studied for our pixel structure with a buried overflow path under the transfer gate. The formula for the PDFWC derived from a simple analytical model has been successfully validated by the technology computer-aided design (TCAD) device simulation and actual device measurement.

I. INTRODUCTION

High dynamic range (HDR) is one of the most important characteristics of recent CMOS image sensors. To achieve over 100dB DR, a lateral overflow integration capacitor (LOFIC) scheme[1-2] and a triple quantization digital pixel sensor[3-4] have been developed.

In these sensors, one of the factors to define the performance at the mode transition points, such as signal-to-noise ratio and linearity, is PDFWC[1].

During the course of our HDR sensor development, we have found that the PDFWC increases as the incident light intensity increases, as shown in Fig. 1 (a). Also, we have known that PDFWC decreases as the time interval between the exposure end of pulsed light and the signal readout, which is referred to as the charge holding time, increases, as shown in Fig. 1 (b). Pulse timing diagrams to obtain the results shown in Fig. 1 (a) and (b) are shown in Fig. 2.

Though analytical models for such dynamic behaviors of the PDFWC have been proposed in the literatures [5-11], minor modifications are needed for our pixel[3-4], because of its unique structure with the buried overflow path under the transfer gate. In this paper, we attempt to understand both the light intensity dependence and the charge holding time dependence of our PPD pixel by simple analytical modeling, TCAD simulations, and measurements.

II. ANALYTICAL MODEL

Contrary to the conventional PPD pixel structure, a buried overflow path has been implemented in our device [3-4]. Its cross-sectional structure and a potential diagram along the z-z' line are shown in Fig. 3. In this structure, the previously reported PDFWC models[5-11] are not applied as they are. The simple model for theoretical analysis is shown in Fig. 4, where three components, the photo-generated current I_{ph}, the intrinsic diode current I_{PPD}, and the overflow current I_{of}, are considered[6].

Models which present the basic concept of our analysis are shown in Figs. 5 and 6. Fig. 5 shows potential changes from the PD reset to high illuminance PD saturation with static light, and Fig. 6 shows potential changes from high illuminance PD saturation to the equilibrium with long t_{hold}.

a. Light Intensity Dependence

Referring to Figs. 3 and 4, formulae for the light intensity dependence of PDFWC will be derived. The photo-generated current I_{ph} and the intrinsic PD current I_{PPD} are formulated, respectively, by

$$I_{ph} = q \cdot R \cdot P \quad \text{-(1)}$$

where q, R and P denote the unit electron charge, the responsivity, and the face-plate illuminance, respectively, and

$$I_{PPD} = I_{sat} \cdot \left\{ e^{\left(\frac{-V_S}{V_T}\right)} - 1 \right\} \quad \text{-(2)}$$

where I_{sat}, V_S, and V_T are the PN junction current at reverse bias condition, the PD potential, and the thermal voltage ($=kT/q$), respectively. If we assume the reverse bias condition with $|V_S| \gg V_T$, in eq. (2), I_{PPD} is approximated by $-I_{sat}$. Then, the overflow current I_{of} is formulated by

$$I_{of} = I_0 \cdot e^{\left(\frac{-\Delta V_b}{n \cdot V_T}\right)} \quad \text{-(3)}$$

where ΔV_b, I_0, and n denote the barrier height between the PD and the overflow path (i.e., $V_S - V_{of}$), the overflow current that would flow at $\Delta V_b = 0$, and the non-ideality factor, respectively. Under the PD saturation conditions, the input and the output currents should be balanced. Therefore, the following relationship holds.

$$I_{ph} = I_{of} + I_{PPD} \quad \text{-(4)}$$

From eq. (1)-(4), the minimum PD potential under PD saturation is given by

$$V_{S\_min} = V_{of} - n \cdot V_T \cdot ln\left(\frac{I_{sat}}{I_0} + \frac{qR}{I_0}P\right) \quad \text{-(5)}$$

Eq. (5) shows that V_{S_min} decreases to flow larger I_{of} when I_{ph} increases.

On the other hand, PDFWC is expressed as

$$N_{FWC} = \frac{C_{PD}}{q}\left(V_{pin} - V_{S\_min}\right) \quad \text{-(6)}$$

From eq. (5) and (6), PDFWC is given by

$$N_{FWC} = \frac{C_{PD}}{q}\left\{V_{pin} - V_{of} + n \cdot V_T \cdot ln\left(\frac{I_{sat}}{I_0} + \frac{qR}{I_0}P\right)\right\} \quad \text{-(7)}$$

Therefore, PDFWC is a function of face-plate illuminance *P*, and it increases logarithmically with the face-plate illuminance. The equilibrium PDFWC[6-8], N_{FWC_eq}, for our pixel structure is obtained from eq. (7) with $P=0$.

$$N_{FWC\_eq} = \frac{C_{PD}}{q}\left\{V_{pin} - V_{of} + n \cdot V_T \cdot ln\left(\frac{I_{sat}}{I_0}\right)\right\} \quad \text{-(8)}$$

The equilibrium PDFWC is PDFWC with the equilibrium condition between the n-layer and the V_{of} barrier of PD.

b. Holding Time Dependence

As shown in Fig. 2(b), $I_{ph} = 0$ during t_{hold}. The PD potential change during t_{hold} is formulated by

$$\frac{dV_S}{dt} = \frac{I_{out}}{C_{PD}} - \frac{I_{in}}{C_{PD}} = \frac{(I_{of}+I_{PPD})}{C_{PD}} - \frac{I_{ph}}{C_{PD}} = \frac{I_0 \cdot e^{\left(\frac{-\Delta V_b}{n \cdot V_T}\right)} - I_{sat}}{C_{PD}} \quad \text{-(9)}$$

Solving eq. (9) yields the PD potential as

$$V_S = V_{of} + n \cdot V_T \cdot \ln\left\{e^{\left(-\frac{I_{sat}}{C_{PD} \cdot n \cdot V_T}t + A\right)} + \frac{I_0}{I_{sat}}\right\} \quad \text{-(10)}$$

where *A* is a constant. With eq. (6), PDFWC is obtained as

$$N_{PD} = \frac{C_{PD}}{q}\left[V_{pin} - V_{of} - n \cdot V_T \cdot \ln\left\{e^{\left(-\frac{I_{sat}}{C_{PD} \cdot n \cdot V_T}t + A\right)} + \frac{I_0}{I_{sat}}\right\}\right] \quad \text{-(11)}$$

Therefore, PDFWC is a function of the charge holding time $t(=t_{hold})$, which demonstrates PDFWC has charge holding time dependence. When t is very long, eq. (10) becomes

$$V_S = V_{S\_long} = V_{of} - n \cdot V_T \cdot \ln\left(\frac{I_{sat}}{I_0}\right) \quad \text{-(12)}$$

From eq. (6) and (12),

$$N_{PD\_long} = \frac{C_{PD}}{q}\left\{V_{pin} - V_{of} + n \cdot V_T \cdot \ln\left(\frac{I_{sat}}{I_0}\right)\right\} \quad \text{-(13)}$$

Eq. (13) is identical to eq. (8), which demonstrates the PDFWC after long t_{hold} (N_{PD_long}) also reaches N_{FWC_eq}. The potential changes during this process are shown in Fig. 6. During the charge holding period, I_{of} draws the charges from PD to FD and finally I_{of} becomes equal to I_{sat}, reaching the equilibrium condition.

III. EXPERIMENTAL VALIDATION

The simulation set-up, simulated $I_{of} - \Delta V_b$ curves, and potential along the x–x' line as a function of the PD potential V_S, are shown in Fig. 7 (a), (b), and (c), respectively. In this simulation, electrons are injected into PD from the inserted PD electrode. With these $I_{of} - \Delta V_b$ curves, the relation between ΔV_b and I_{of} was confirmed.

Fig. 8(a) shows another simulation set-up for light intensity dependence (Fig. 9) and charge holding time dependence (Fig. 10) of PDFWC. The PD electrons are generated by an external light source in this simulation. Fig. 8(b) shows the photo-response curve. In the PD saturation region, it is obvious that eq. (4) holds with $I_{of} \gg I_{PPD}$.

Fig. 9 shows the light intensity dependence of PDFWC and PD potential. The simulation result of (a) and eq. (5) agree well, and the simulation result of (b) and eq. (7) reproduce the measurement result.

Fig. 10 shows the t_{hold} dependence. The simulation result of (a) agrees well with eq. (10). Eq. (11) reproduces the measurement result, as shown in (b). Figs. 9(c) and 10(c) show potential changes from PD reset to PD saturation and potential changes from PD saturation to equilibrium PDFWC, respectively. The black and dashed gray lines show the PD potentials under the fully depleted condition, and low illuminance saturation or after a long t_{hold}, respectively.

The potential distributions at low illuminance saturation and after long t_{hold}, as shown with the dashed gray lines of Fig. 9(c) and Fig. 10(c), are re-plotted in Fig. 11. It is understood that the equilibrium PDFWC condition is reached in both cases.

IV. CONCLUSION

In this paper, the light intensity dependence of PDFWC and the PD charge reduction phenomenon during the charge holding time have been formulated. They were verified with TCAD simulations and measurement results for our pixel with a buried overflow path. During the charge integration period, electrons flowing into and those flowing out from the PD should be balanced. Therefore, the potential barrier between the PD and the overflow path is a function of input light intensity. It decreases with the light intensity logarithmically, increasing the PDFWC logarithmically. For both cases where the signal charges remain in the PD at dark before they are read out, and where the light intensity is close to zero, PDFWC becomes identical to the equilibrium FWC.

V. ACKNOWLEDGMENT

The authors gratefully acknowledge Meta Reality Labs and TSMC for the sensor development.

REFERENCES

[1] N. Akahane et al., IEEE Trans. Elec. Dev., 56, 11, pp. 2429-2435, 2009.

[2] I. Takayanagi et al., MDPI Sensors, 19, 5572, 2019.

[3] C. Liu et al., IEDM2020, pp. 327-330, 2020

[4] R. Ikeno et al., IISW2023, P44, 2023.

[5] M. Sarkar et al., IEEE Trans. Elec. Dev., 60, 3, pp.1154-1161, 2013.

[6] A. Pelamatti et al., IEEE Elec. Dev. Let., 34, 7, pp. 900-902, 2013.

[7] V. Goiffon et al., IEEE J. of the Elec. Dev., Society, 2, 4, 2014.

[8] A. Pelamatti et al., IEEE Trans. Elec. Dev., 62. 4. pp. 1200-1207, 2015.

[9] Z. Gao et al., IEEE Sensors Journal, 16, 8, pp. 2367-2373, 2016.

[10] H. Alaibakhsh, et al., IEEE Trans. Elec. Dev., 65, 10, pp. 4362-4368, 2018.

[11] J. Cao et al., Journal of the EDS, 8, pp. 1063-1071, 2020.

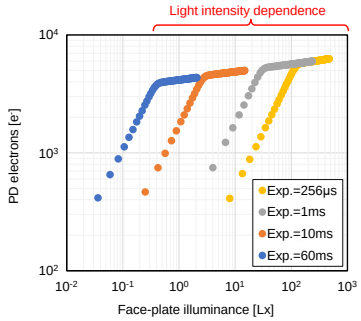

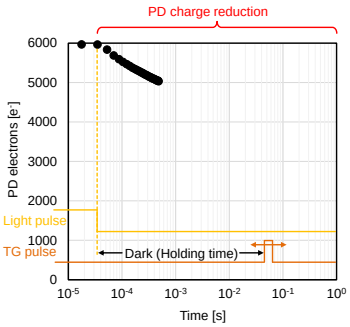

(a)Photo-conversion characteristics (b) PDFWC dependence on the t_{hold}

Fig. 1 Measured dynamic behaviors of PPD.

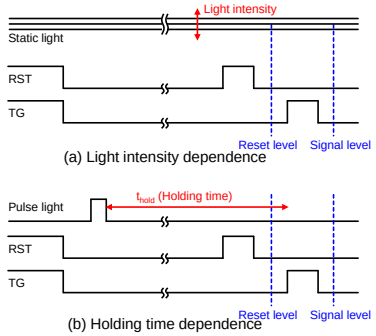

Fig. 2 Pulse timing for evaluation.

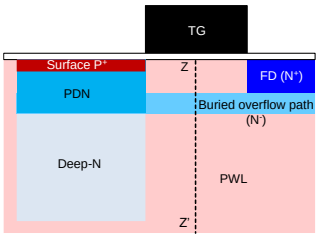

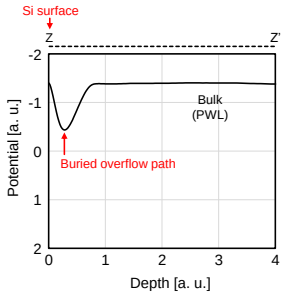

Fig. 3 PD cross-section and potential of the buried overflow path.

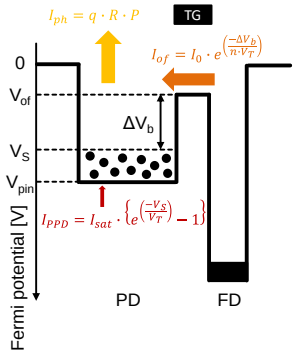

Fig. 4 Simple model for theoretical analysis.

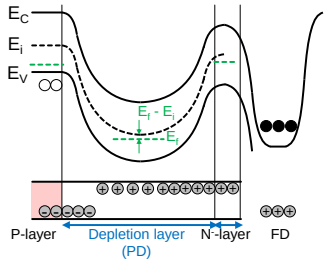

(a) Fully depleted

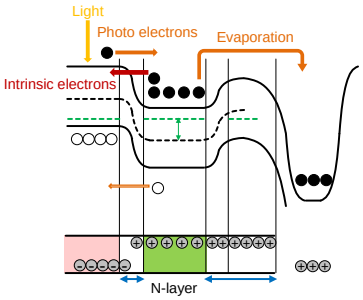

(b) Low illuminance saturation (~Equilibrium saturation)

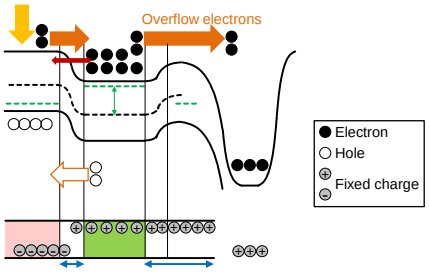

(c) High illuminance saturation

Fig. 5 A simple model of potential changes from PD reset to PD saturation.

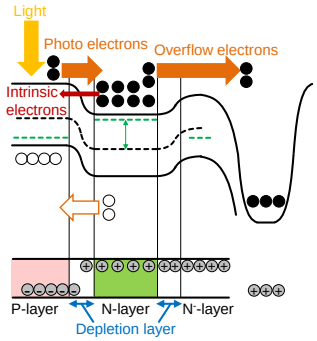

(a) High illuminance saturation

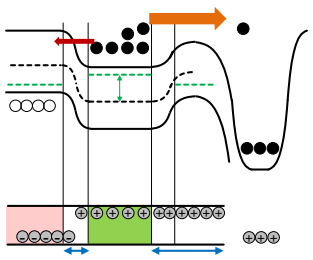

(b) During holding time

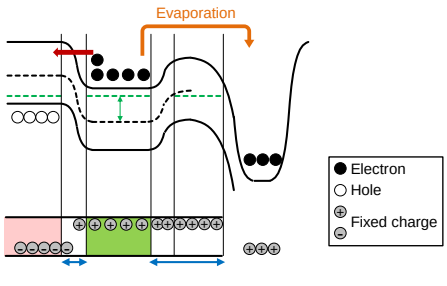

(c) Equilibrium saturation

Fig. 6 A simple model of potential changes from PD saturation to equilibrium PDFWC.

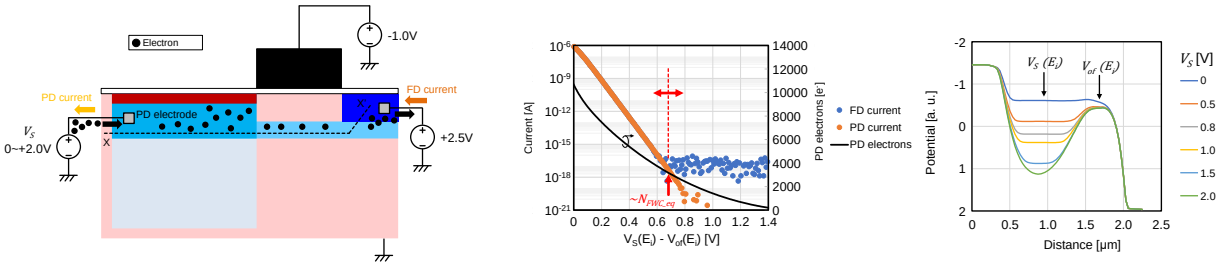

(a) TCAD simulation set-up of $I_{of} - \Delta V_b$ (b) $I_{of} - \Delta V_b$ curve result (c) Potential of each V_S voltage

Fig. 7 Relation between ΔV_b and I_{of} with TCAD simulation.

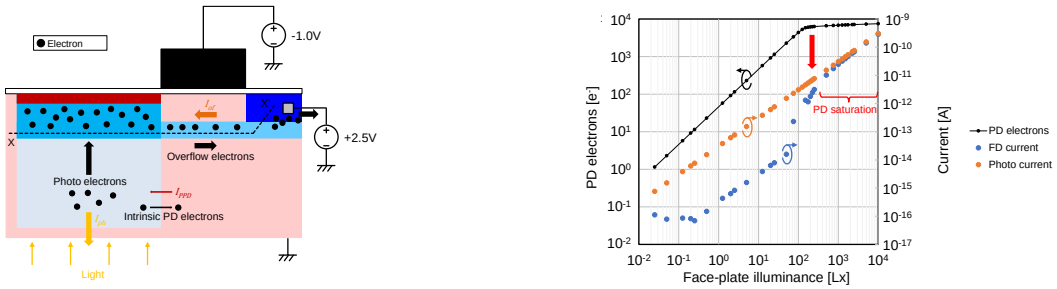

(a) TCAD simulation set-up (b)Photo-response curve with TCAD simulation

Fig. 8 TCAD simulation and evaluation set-up for light intensity (Fig. 9) and charge holding time (Fig. 10) dependence.

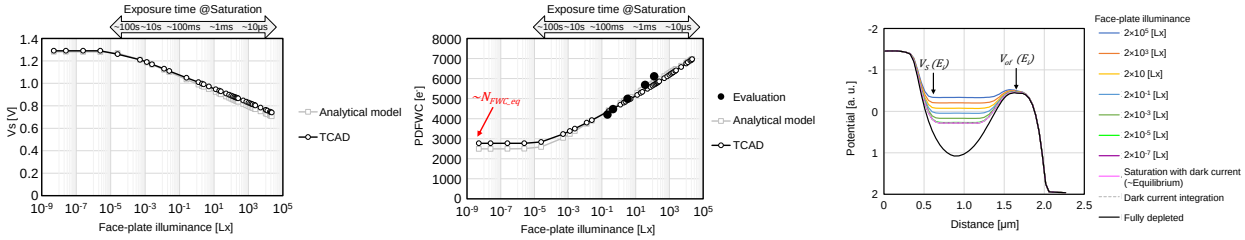

(a) PD potential (b) PDFWC (c) Potential of saturation with low and high P

Fig. 9 PDFWC with various light intensity conditions.

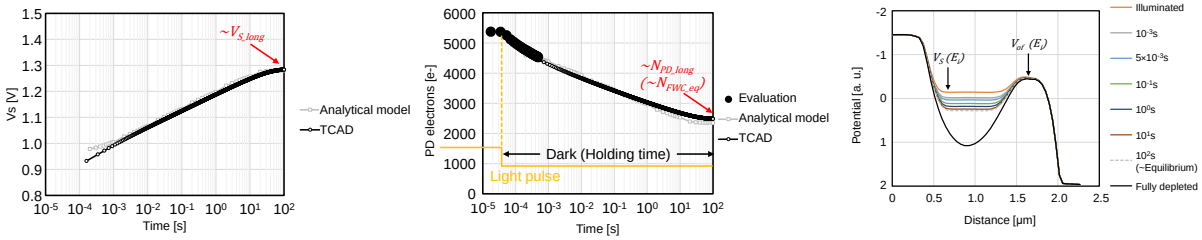

(a) PD potential (b) PD electrons (c) Potential with several t_{hold}

Fig. 10 PDFWC with long charge holding time.

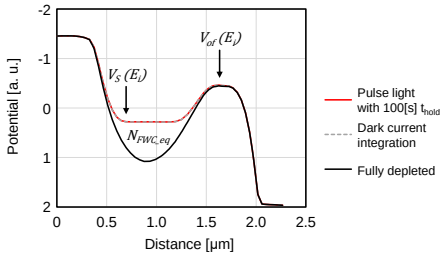

Fig. 11 Equilibrium PDFWC potential with TCAD